Downlink Capacity of Two-tier Cognitive Femto Networks

Shin-Ming Cheng, Weng Chon Ao, and Kwang-Cheng Chen
Graduate Institute of Communication Engineering, National Taiwan University, Taipei 106, Taiwan
Email: smcheng@cc.ee.ntu.edu.tw, r97942044@ntu.edu.tw, and chenkc@cc.ee.ntu.edu.tw

***Abstract*—In two-tier networks consisting of a macrocell overlaid with femtocells in co-channel deployment and closed-access policy, spatial reuse is achieved at the price of severe cross-tier interference from concurrent transmissions. The lack of direct coordination between the macro and femtocells makes interference control as a challenging issue. Cognitive radio (CR) becomes a promising solution, where femtocells with cognitive information accomplish concurrent transmissions while meeting a per-tier outage constraint. Several interference-aware allocation approaches are proposed to enhance spatial reuse according to cognitive capabilities of femtocell. By employing stochastic geometry model, bounds on the distribution of aggregated interference from two-tier spatial point processes are successfully analyzed. The maximum number of simultaneously transmitting femtocells and overall downlink capacity of two-tier networks meeting a per-tier outage requirement in each approach are theoretically derived. This paper proves that with stronger cognitive capability (i.e., more knowledge interpreted) at femtocell, more spatial reuse gain can be found.**

I. Introduction

Two-tier femtocell networks have received tremendous attention in recent years because of providing in-building coverage for indoor users via femtocell base stations (femto-BSs) to complement the poor signal from the macrocell BS (macro-BS). With the small coverage area, femtocells also facilitate large number of concurrent transmissions that can be accommodated in the network, which improves spatial reuse, therefore potentially yielding enhanced wireless capacity.

To effectively exploit scarce resources, the *co-channel* deployment is widely adopted, where macrocells and femtocells are operated in a common spectrum. Obviously, heavy *cross-tier interference* is introduced where macrocell and femtocell play the role of either the aggressor or the victim. Since femto-BSs are paid for, deployed by, and maintained by the customers, instead of allowing all users to connect, *closed-access* policy is adopted where only mobile subscribers of femto-BS (femto-MSs) are allowed to establish connection. This introduces more severe cross-tier interference since femto-MS will be disturbed by passing unauthorized users who connected with macro-BS (abbrev. as macro-MS) in vicinity. As a result, the destructive interference incurred by spatial reuse might limit the capacity improvement benefited by concurrent transmissions and thus many works investigated the interference control problem [1]–[5].

However, the ad-hoc nature of femto-BS deployments implies that no direct coordination for interference control exists between macro-BS and femto-BS. On the other hand, the indirected coordination via wired backbone introduces long delay [3] and is infeasible to mitigate interference. Therefore, decentralized strategies for interference management may be more appropriated [1], [3]–[7]. Our previous work [7] firstly introduced the concept of cognitive radio (CR) for interference mitigation, where femto-BS being capable of CR functionality can sense the received signaling from macro-BS and allocate resource without impacting macro-MSs in a more intelligent way.

In this paper, the knowledge granularity interpreted from cognitive information is classified into two categories according to the CR capability of femto-BS, that is, *resource* level and *user* level. In the former level, femto-BS identifies if a resource is occupied, and thus can simply avoid to allocate the occupied resource to eliminate the interference (known as *interweave* approach). To achieve spatial reuse, *underlay* approach is proposed where concurrent two tier transmissions may occur as long as the aggregated cross-interference incurred by femto-BSs is below some acceptable constraint. If the femto-BS is capable of cognizing *user* level information, for example, the specific macro-MS allocated to a resource or the location in which the assigned macro-MS will use a resource [3], *controlled underlay* approach is adopted where femto-BS prevents using the resources allocated for the macro-MS in vicinity and spatial reuse is further improved.

This paper provides theoretical results on the downlink capacity of two-tier femtocell networks under different allocation approaches and thus is different from the similar works focused on uplink capacity [4] or cellular ad hoc network [8], [9]. By employing stochastic geometry model, bounds on the distribution of aggregated interference from two-tier spatial point processes are successfully analyzed. The maximum femto-BS density and thus maximum overall capacity satisfying a per-tier outage constraint can be characterized.

The remainder of this paper is organized as follows. Section II presents the system model, CR models and access approaches. In Section III, we analyze the overall capacities in different access approaches. Numerical results are provided along the discussions. Section IV concludes this paper.

II. System Model

This section describes the network being considered and the models being applied. The assumptions made in this paper are also justified.

978-1-4244-8015-9/10/$26.00 ©2010 IEEE

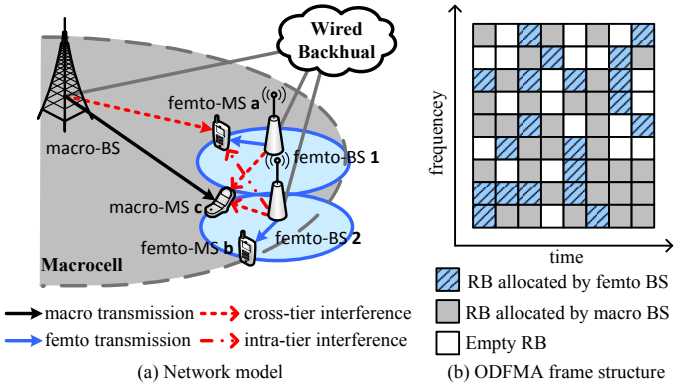

Fig. 1. Macro/femto networks deployment

A. Two-tier Network Architecture

As shown in Fig. 1 (a), the downlink of an orthogonal frequency division multiple access (OFDMA) system with two-tier macro- and femtocells is considered. As shown in Fig. 1 (b), OFDMA-based systems typically divide system bandwidth into N basic time-frequency units of resource blocks (RBs). To achieve universal frequency reuse, both macro- and femtocells utilize the all RBs, which is known as the *co-channel* deployment. The *closed access* policy is assumed, where only subscribed femto-MS is allowed to be served by femto-BS. The unauthorized macro-MS can only be served by macro-BS even it locates within the femtocell coverage. Macro- and femto-BS respectively transmit to only one user at any given RB at full power P_m and P_f, which implies transmission power is maintained constant across the RBs. Perfect synchronization in time and frequency is assumed.

Denote $\mathcal{H} \in \mathbb{R}^2$ as the interior of a reference macrocell of radius R_m, which consists of multiple macro-MSs and a macro-BS located in central of $\mathcal{H}$. The spatial distribution of macro-MSs is assumed to follow a homogeneous Poisson Point Process (PPP) with density μ_m, and the locations of the macro-MSs are denoted as $\Phi_m = \{X_i\}$. The macrocell is overlaid with femto-BSs of radius R_f, which are randomly distributed on $\mathbb{R}^2$ according to a homogeneous PPP with intensity λ_f. We let $\Phi_f = \{Y_i\}$ denote the locations of the femto-BSs. As will be needed in the following analysis, subset of femto-BSs, denoted as $\Phi_f^p = \{Y_i : B_i(p) = 1\}$ with node density $p\lambda_f$, is always obtained by independent thinning of Φ_f with probability p, where $B_i(p)$ are i.i.d. Bernoulli random variables with parameter p.

The signal propagation in this paper is assumed to decay empirically with distance d between transmitter and receiver. Please note that this paper denotes $\mathcal{B}(v; r)$ as the circle of radius r centered at node v and $\mathbb{P}[\mathcal{E}]$ as the probability of event $\mathcal{E}$ occurs.

B. CR Capability at Femto-BS

As shown in Fig. 1 (a), no direct coordination exists between femto-BS and macro-BS on the wireless edge. Moreover, the unacceptable delay on the wired connection between them makes real-time coordination impossible. With CR capability, femto-BS could acquire information of macrocell without or with minimum assistances from macro-BS. The knowledge granularity interpreted from cognitive information is classified into two categories according to the cognitive capability of femto-BS as follows.

Resource level information. By adopting traditional spectrum sensing techniques, the detection of the femto-BS signals can be achieved without any coordination. If the received interference power of a RB, e.g., RSRP (Reference Signal Received Power) in LTE network, exceeds a certain threshold, femto-BS identifies that the RB is occupied by macro-MS [7].

User level information. User level information indicates the knowledge related to the behavior of a macro-MS, such as the specific macro-MS allocated to a RB or the location in which the assigned macro-MS will use a RB. Typically, such scheduling or zone allocation information [5] is encapsulated in PDCCH (LTE) or DLMAP (WiMax) by encoding with identities of served MSs. We can simply assign femto-BSs a special user identity for decoding such information broadcast channel.

C. Allocation Approaches of Cognitive Femto-BS

With different levels of cognitive capabilities, femto-BS adopts different allocation approaches [10] to achieve different levels of spatial reuse.

Interweave approach. With resource level information, femto-BS acting as secondary user can passively seek temporary frequency voids of RBs for opportunistic allocation. Consequently, femto-MSs and macro-MSs are operating on orthogonal RBs, and no cross-tier interference is introduced. However, this approach restricts the system capacity since no spatial reuse is adopted.

Underlay approach. Comparing with the interweave approach, femto-BSs in this approach aggressively exploit RBs occupied by macro-MSs to increase spatial reuse as long as resulting aggregated cross-interference is lower than the outage constraint. However, with resource level information, femto-BS is unable to distinguish whether the occupied RBs are assigned to the macro-MSs in its vicinity, and has to assume the worse case. That is, the femto transmission should ensure the outage constraint of all macro-MSs that may occupy the RB. Thus, there is no appreciable gain from spatial reuse due to the overestimation.

Controlled underlay approach. If a femto-BS is able to leverage macro-MS user level scheduling or location information, the femto-BSs are able to determine the set of RBs that can be reused without causing (to macro-MSs in their vicinity) interference. By deactivating the femto-BSs on the RBs dedicated to a neighboring macro-MS, more concurrent femto transmissions are allowed and the overall capacity is increased.

D. Metrics of Internet

This paper controls the active femto-BS density to guarantee the aggregated intra- or cross-tier interference satisfying a per-tier outage constraint. The capacity computed as the product of the density of successful two tier transmissions and the data rate with an outage constraint should achieve maximum fairness. More specifically, this capacity is given by the maximum uniform throughput, which is defined as the minimum of the achieved throughputs, considering all MSs in the network.

III. Interference Modeling

This section analyzes the impact of received interference in either tier MS on the overall capacity under three allocation approaches.

A. Interweave approach

With resource level information such as RB allocation usage of the overlaid macrocell, femto-BS can identify the RBs occupied by macro-MS (denoted as macro RBs) and empty RBs available for allocation (denoted as empty RBs). The sets of macro and empty RBs are denoted by $\mathcal{N}_m$ and $\mathcal{N}_e$, respectively.

In this approach, macro- and femto-BSs orthogonally allocate RBs for MSs, thus we respectively discuss the interference received in macro-MS at a macro RB and femto-MS at an empty RB. The received Signal-to-interference-plus-noise ratio (SINR) observed by a macro-MS at a macro RB amounts to

$$\gamma_m = \frac{G_m P_m r_m^{-\alpha}}{N_0}, \tag{1}$$

where G_m is the channel gain for macro-MS and is supposed to be exponential distributed with unit mean, α is the path loss exponent, N_0 is the background noise power per RB, and r_m is the distance between the macro-BS and the macro-MS. Under the near-far effect of macrocell, to guarantee the QoS for all macro-MSs, γ_m received at the macro-MS located at the edge of the serving area (i.e., $r_m = R_m$) shall satisfy

$$\mathbb{P}\left(\frac{G_m P_m R_m^{-\alpha}}{N_0} \geq \Gamma\right) \geq 1-\epsilon, \tag{2}$$

where Γ is the SINR threshold of a MS, and an outage constraint is imposed on the MS with a maximum outage probability ϵ. The equality holds when the serving area exactly matches the cell coverage. Here the serving area is smaller than the cell coverage to account for extra interference tolerance. The normalized maximum downlink capacity of macrocell network C_m at a macro RB is derived by using the Shannon capacity formula as

$$C_m^{\text{inter}} = \log_2(1+\Gamma). \tag{3}$$

Regarding femto-MS, the received SINR γ_f at an empty RB is $\gamma_f = \frac{G_f P_f r_f^{-\alpha}}{N_0 + I_{f,f}}$, where G_f accounts for the channel gain and is supposed to be exponential distributed with unit mean, r_f is the distance between a femto-MS and its serving femto-BS, and $I_{f,f}$ is the intra-tier interference defined later. Similar to the considerations in macrocell, γ_f of a femto-MS located at the cell boundary of its serving femto-BS (i.e., $r_f = R_f$) shall guarantee

$$\mathbb{P}\left(\frac{G_f P_f R_f^{-\alpha}}{N_0 + I_{f,f}} \geq \Gamma\right) = 1-\epsilon, \tag{4}$$

where $I_{f,f} = \sum_{Y_i \in \Phi_f^{\hat{p}} \setminus \{Y_0\}} G_{Y_i} P_f \|Y_i\|^{-\alpha}$ is the intra-tier interference from surrounding femto-BSs to a typical (reference) femto-MS located at the origin. By the stationary characteristic of homogeneous Poisson point process [11], the interference measured by the typical femto-MS is representative of the interference seen by all other femto-MSs. G_{Y_i} and $\|Y_i\|$ are respectively the channel gain and the distance between the femto-BS at Y_i and the typical femto-MS at the origin. The femto-BS at Y_0 is the serving BS for the reference femto-MS. From [12], the moment generating function of $I_{f,f}$ is

$$\begin{aligned}\mathbb{E}[\exp(-sI_{f,f})] &= \exp\left(-2\pi\widehat{\lambda}_f \int_0^\infty \frac{u}{1+\frac{u^\alpha}{sP_f}} du\right) \\ &= \exp\left(-\widehat{\lambda}_f P_f^{2/\alpha} s^{2/\alpha} K_\alpha\right),\end{aligned} \tag{5}$$

where $K_\alpha = \frac{2\pi^2}{\alpha \sin(2\pi/\alpha)}$, and $\widehat{\lambda}_f$ is the maximum allowed femto-BS density. To derive $\widehat{\lambda}_f$, the left hand side of (4) can be evaluated as

$$\begin{aligned}&\mathbb{P}\left[G_f \geq \frac{\Gamma}{P_f R_f^{-\alpha}}(N_0 + I_{f,f})\right] \\ &= \exp\left(-\frac{\Gamma}{P_f R_f^{-\alpha}} N_0\right) \exp(-\widehat{\lambda}_f R_f^2 \Gamma^{\frac{2}{\alpha}} K_\alpha).\end{aligned} \tag{6}$$

We thus have

$$\widehat{\lambda}_f = \frac{-\ln(1-\epsilon) - \frac{\Gamma}{P_f R_f^{-\alpha}} N_0}{R_f^2 \Gamma^{\frac{2}{\alpha}} K_\alpha}. \tag{7}$$

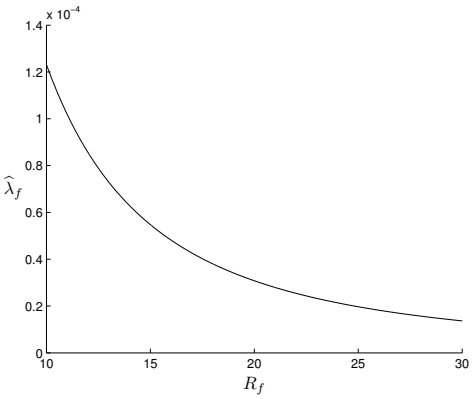

Fig. 2. Effects of R_f on $\widehat{\lambda}_f$

Fig. 2 shows the effects of R_f on $\widehat{\lambda}_f$. $R_f = 15$ is chosen and the corresponding $\widehat{\lambda}_f \approx 5.48 \times 10^{-5}$. The system parameters are set as $N_0 = 10^{-12}$, $\alpha = 4$, $\epsilon = 0.1$, $\Gamma = 3$, $P_f = 0.01$, which are used in all numerical results in the following figures.

The maximum downlink capacity of femtocell network C_e at an empty RB is

$$C_e = \widehat{\lambda}_f \mathcal{H} \log_2(1+\Gamma). \tag{8}$$

Then the maximum total system capacity of the two-tier network C is

$$C^{\text{inter}} = |\mathcal{N}_m| C_m^{\text{inter}} + |\mathcal{N}_e| C_e. \tag{9}$$

B. Underlay approach

In this approach, femto-BSs try to exploit macro RBs to achieve spatial reuse according to resource level information. We control the number of interfering sources (i.e., active femto-BSs) to prevent violating outage constraint at the macro-MS, and the details are described by the following lemmas.

Lemma 1. *To avoid interference from femto-BSs violating the outage constraint at a macro-MS in the macrocell with serving area radius R_m, the active femto-BS density shall not be larger than* $\widetilde{\lambda}_f = \frac{-\ln(1-\epsilon) - \frac{\Gamma}{P_m R_m^{-\alpha}} N_0}{R_m^2 (\frac{\Gamma P_f}{P_m})^{\frac{2}{\alpha}} K_\alpha}$.

Proof: Considering the macro-MS at the serving area edge of the macro-BS, the following outage constraint shall be maintained

$$\mathbb{P}\left(\frac{G_m P_m R_m^{-\alpha}}{N_0 + I_{f,m}} \geq \Gamma \right) = 1 - \epsilon, \tag{10}$$

where $I_{f,m} = \sum_{Y_i \in \Phi_f^{\bar{p}}} G_{Y_i} P_f \|Y_i\|^{-\alpha}$ is the interference contributed from surrounding femto-BSs to the macro-MS. Note that here the cross-tier interference makes the macrocell coverage match its serving area. The left side of (10) can be evaluated as

$$\begin{aligned} &\mathbb{P}\left[G_m \geq \frac{\Gamma}{P_m R_m^{-\alpha}} (N_0 + I_{f,m}) \right] \\ &= \exp\left(-\frac{\Gamma}{P_m R_m^{-\alpha}} N_0 \right) \exp\left(-\widetilde{\lambda}_f R_m^2 \left(\frac{\Gamma P_f}{P_m} \right)^{\frac{2}{\alpha}} K_\alpha \right) \end{aligned} \tag{11}$$

We thus have

$$\widetilde{\lambda}_f = \frac{-\ln(1-\epsilon) - \frac{\Gamma}{P_m R_m^{-\alpha}} N_0}{R_m^2 (\frac{\Gamma P_f}{P_m})^{\frac{2}{\alpha}} K_\alpha}. \tag{12}$$

■

Corollary 1. *The maximum allowed femto-BS density $\widetilde{\lambda}_f$ is a monotonically decreasing function of R_m when QoS requirement of all macro-MSs is satisfied.*

We can easily observe **Corollary 1** from numerical results shown in Fig. 3 where $P_m = 20$. Please note that R_m can be estimated at femto-BS by received power of signal broadcasted from the macro-BS or be set as predefined parameter. $R_m = 500$ is chosen and the corresponding $\widetilde{\lambda}_f \approx 2 \times 10^{-6}$. Another constraint for active femto-BS density can be derived in the respective of femto-MS. When a femto-MS reuses the macro RB to receive data, the received SINR highly depends on the distance between itself and the macro-BS, which is approximate to the distance between the serving femto-BS and

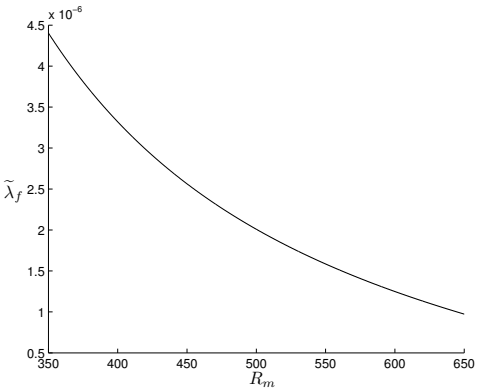

Fig. 3. Effects of R_m on $\widetilde{\lambda}_f$

the macro-BS (denoted as d_f). Moreover, received SINR at the femto-MS is also limited by interference from surrounding femto-BSs, following lemma describes the allowed femto-BS density.

Lemma 2. *To avoid interference from femto-BSs violating the outage constraint at a femto-MS, the active femto-BS density shall not be larger than* $\overline{\lambda}_f = \left(-\ln\left[(1-\epsilon)\left(1 + \frac{\Gamma P_m \overline{d}_f^{-\alpha}}{P_f R_f^{-\alpha}} \right) \right] - \frac{\Gamma}{P_f R_f^{-\alpha}} N_0 \right) / (R_f^2 \Gamma^{\frac{2}{\alpha}} K_\alpha)$.

Proof: To guarantee the outage constraint, a femto-MS located at the cell boundary of its serving femto-BS with the shortest distance to macro-BS (denoted as $\overline{d}_f$) should be considered since it suffers the most severe cross-tier interference. The following equation shall be satisfied at this femto-MS.

$$\mathbb{P}\left(\frac{G_f P_f R_f^{-\alpha}}{N_0 + \overline{I}_{m,f} + I_{f,f}} \geq \Gamma \right) = 1 - \epsilon, \tag{13}$$

where $\overline{I}_{m,f} = G_m P_m (\overline{d}_f)^{-\alpha}$ is the approximate cross-tier interference from the macro-BS to the femto-MS, which is located at the cell boundary of the femto-BS with distance $\overline{d}_f$ away from the macro-BS. The left side of (13) can be evaluated as

$$\begin{aligned} &\mathbb{P}\left[G_f \geq \frac{\Gamma}{P_f R_f^{-\alpha}} (N_0 + \overline{I}_{m,f} + I_{f,f}) \right] \\ &= \exp\left(-\frac{\Gamma}{P_f R_f^{-\alpha}} N_0 \right) \left(\frac{1}{1 + \frac{\Gamma P_m \overline{d}_f^{-\alpha}}{P_f R_f^{-\alpha}}} \right) \exp\left(-\overline{\lambda}_f R_f^2 \Gamma^{\frac{2}{\alpha}} K_\alpha \right). \end{aligned} \tag{14}$$

Thus we have

$$\overline{\lambda}_f = \frac{-\ln\left[(1-\epsilon)\left(1 + \frac{\Gamma P_m \overline{d}_f^{-\alpha}}{P_f R_f^{-\alpha}} \right) \right] - \frac{\Gamma}{P_f R_f^{-\alpha}} N_0}{R_f^2 \Gamma^{\frac{2}{\alpha}} K_\alpha}. \tag{15}$$

■

Corollary 2. *Satisfying QoS requirement of all femto-MS requires the maximum allowed femto-BS density to be a monotonically increasing function of $\overline{d}_f$, as shown in Fig. 4.*

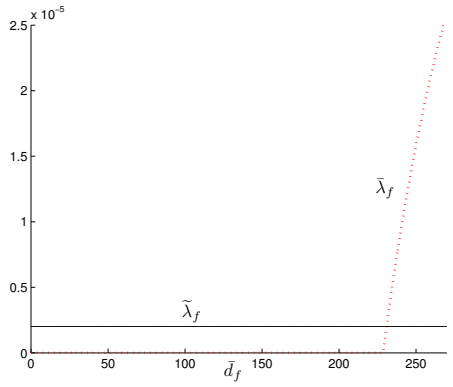

Fig. 4. $\widetilde{\lambda}_f$, $\overline{\lambda}_f$, and corresponding $\breve{\lambda}_f$ over different $\overline{d}_f$

Please note that to compute $\overline{\lambda}_f$ at each femto-BS in a distributed fashion, $\overline{d}_f$ shall be firstly retrieved. By either exchanging its own d_f with neighboring femto-BS, $\overline{d}_f$ can be easily determined. Or macro-BS can record d_f for all femto-BSs and periodically broadcast to every femto-BS. Each femto-BS exploits the next lemma to determine the maximum allowed femto-BS density (and thus the access probability of a femto-BS on a marco RB) to guarantee QoS of both macro- and femto-MSs.

Lemma 3. *Under the situation that R_m and $\overline{d}_f$ are known, to guarantee QoS of both macro- and femto-MSs, the maximum allowed femto-BS density at a macro RB (denoted as $\breve{\lambda}_f$) for the two-tier network equals* $\min(\widetilde{\lambda}_f, \overline{\lambda}_f)$

Fig. 4 shows $\widetilde{\lambda}_f$, $\overline{\lambda}_f$ and corresponding $\breve{\lambda}_f$ under different $\overline{d}_f$ with parameter setups $R_f = 15$ and $R_m = 500$. (12) indicates that $\widetilde{\lambda}_f$ does not affected by $\overline{d}_f$ and remains as a constant. Please note that the femto-MSs with d_f smaller than a threshold d_f^t (about 230) can not allow any intra-interference from surrounding femto-BSs since cross-interference from macro-BS already make femto-MS violate outage constraint. Thus, we observe that $\overline{\lambda}_f = 0$ when $\overline{d}_f \leq d_f^t$.

Corollary 3. *If $\breve{\lambda}_f = \overline{\lambda}_f$, the serving area radius of macro-BS may be extended from R_m to $R_m^u = \sqrt{\frac{-\ln(1-\epsilon)}{K_\alpha(\frac{\Gamma P_f}{P_m})^{\frac{2}{\alpha}}\overline{\lambda}_f}}$.*

Proof: When $\breve{\lambda}_f = \overline{\lambda}_f$, **Lemma 3** implies $\breve{\lambda}_f \leq \widetilde{\lambda}_f$ and (11) becomes

$$\mathbb{P}\left[G_m \geq \frac{\Gamma}{P_m R_m^{u\,-\alpha}}(N_0 + I_{f,m})\right] = \exp\left(-\frac{\Gamma}{P_m R_m^{u\,-\alpha}}N_0\right)\exp\left(-\breve{\lambda}_f R_m^{u\,2}\left(\frac{\Gamma P_f}{P_m}\right)^{\frac{2}{\alpha}}K_\alpha\right) \quad (16)$$

In the interference limited regime, we set $N_0 = 0$ and have,

$$R_m^u = \sqrt{\frac{-\ln(1-\epsilon)}{K_\alpha\left(\frac{\Gamma P_f}{P_m}\right)^{\frac{2}{\alpha}}\breve{\lambda}_f}}. \quad (17)$$

Obviously, as the active femto-BS density decreases, the corresponding serving area radius of macro-BS increases followed **Corollary 1**. ■

Corollary 4. *If $\breve{\lambda}_f = \widetilde{\lambda}_f$, each active femto-BS coverage radius may be extended from R_f to R_f^u.*

Proof: When $\breve{\lambda}_f = \widetilde{\lambda}_f$, **Lemma 3** implies $\breve{\lambda}_f \leq \overline{\lambda}_f$ and (14) becomes

$$\mathbb{P}\left[G_f \geq \frac{\Gamma}{P_f R_f^{u-\alpha}}(N_0 + \overline{I}_{m,f} + I_{f,f})\right] = \exp\left(-\frac{\Gamma}{P_f R_f^{u-\alpha}}N_0\right)\left(\frac{P_f R_f^{u-\alpha}}{P_f R_f^{u-\alpha} + \Gamma P_m \overline{d}_f^{-\alpha}}\right) \times \exp\left(-\breve{\lambda}_f R_f^{u2}\Gamma^{\frac{2}{\alpha}}K_\alpha\right). \quad (18)$$

R_f^u does not have closed-form generally and can be solved numerically. As can be seen from (15), when active femto-BS density decreases, the femto-BS coverage radius increases. ■

The system capacity at a macro RB supported by one macro-BS and $\breve{\lambda}_f\mathcal{H}$ femto-BSs becomes

$$C_m^{\text{under}} = (\breve{\lambda}_f\mathcal{H} + 1)\log_2(1+\Gamma). \quad (19)$$

The overall capacity C^{under} can be derived by substituting C_m^{inter} in (9) with C_m^{under}.

C. Controlled-underlay approach

When the user level scheduling or geographical information at each RB is known by a femto-BS, the femto-BS is able to determine whether a macro-MS detected within its sensing area (with radius r_s) currently occupies an RB. Then the femto-BS may deactivate itself at the corresponding RBs occupied by the detected macro-MSs to eliminate its dominant cross-tier interference. The overall capacity may thus increase. This approach implies that femto-BSs located within radius r_s of a macro-MS will be deactivated at the RB occupied by the macro-MS; in other words, each macro-MS has an *avoidance region* with radius r_s. Following lemma describes the effect of *avoidance region* on allowable femto-BS density.

Lemma 4. *When all femto-BSs located in the avoidance region with radius r_s of a macro-MS are deactivated at the RB occupied by the macro-MS, the allowable femto-BS density $\widetilde{\lambda}'_f$ is larger than that without introducing avoidance region, i.e., $\widetilde{\lambda}_f$ in **Lemma 1**.*

Proof: The interference from surrounding femto-BSs at a typical macro-MS located at origin becomes

$$I_{f,m}^{\text{c-under}} = \sum_{Y_i \in \Phi_f^{\bar{p}'} \setminus \mathcal{B}(0;r_s)} G_{Y_i} P_f \|Y_i\|^{-\alpha}. \quad (20)$$

The moment generating function of $I_{f,m}^{\text{c-under}}$ is

$$\mathbb{E}\left[\exp\left(-sI_{f,m}^{\text{c-under}}\right)\right] = \exp\left(-2\pi\widetilde{\lambda}'_f\int_{r_s}^{\infty}\frac{u}{1+\frac{u^\alpha}{sP_f}}du\right) \quad (21)$$

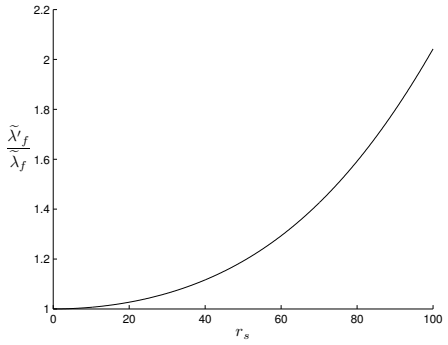

Fig. 5. Spatial reuse improvement under different radius r_s setups for avoidance region

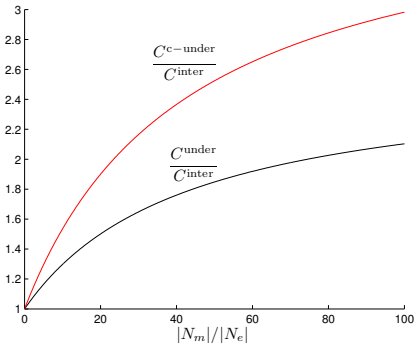

Fig. 6. Overall capacity gain from spatial reuse under different $|\mathcal{N}_m|/|\mathcal{N}_e|$

Substitute $s = \frac{\Gamma}{P_m R_m^{-\alpha}}$ and $\alpha = 4$ in (21), we have

$$\mathbb{E}\left[\exp\left(-\frac{\Gamma}{P_m R_m^{-\alpha}} I_{f,m}^{\text{c-under}}\right)\right]$$
$$= \exp\left\{-\widetilde{\lambda}'_f R_m^2 \left(\frac{\Gamma P_f}{P_m}\right)^{\frac{1}{2}} \left[\frac{\pi^2}{2} - \pi \tan^{-1}\left(\sqrt{\frac{P_m}{\Gamma P_f}} \frac{r_s^2}{R_m^2}\right)\right]\right\}$$

Comparing the allowed femto-BS density to that without avoidance region by applying $\alpha = 4, K_4 = \pi^2/2$ in (12). We have the following ratio

$$\frac{\widetilde{\lambda}'_f}{\widetilde{\lambda}_f} = \frac{\pi^2/2}{\pi^2/2 - \pi \tan^{-1}\left(\sqrt{\frac{P_m}{\Gamma P_f}} \frac{r_s^2}{R_m^2}\right)} \geq 1. \quad (22)$$

(22) shows the increase of allowed femto-BS density when avoidance region is introduced. ■

Intuitively, by importing an avoidance region, we prevent the event that the interference from a single dominant femto-BS causes outage reception at a macro-MS. Fig. 5 describes (22) and shows that the spatial reuse improves as r_s increases.

Similar to **Lemma 3**, the maximum allowed femto-BS density at a macro RB (denoted as $\breve{\lambda}'_f$) with avoidance region is $\min(\widetilde{\lambda}'_f, \overline{\lambda}_f)$. The system capacity at a macro RB supported by one macro-BS and $\breve{\lambda}'_f \mathcal{H}$ femto-BSs becomes

$$C_m^{\text{c-under}} = (\breve{\lambda}'_f \mathcal{H} + 1) \log_2(1 + \Gamma). \quad (23)$$

The overall capacity $C^{\text{c-under}}$ can be derived by substituting C_m^{inter} in (9) with (23). Obviously, following corollary holds.

Corollary 5. *With CR capability at femto-BS, avoidance region is realized and overall system capacity in improved.*

Fig. 6 compares C^{inter}, C^{under}, and $C^{\text{c-under}}$ under different $|\mathcal{N}_m|/|\mathcal{N}_e|$, with $\overline{d}_f = 240$ and $r_s = 90$. It is obviously that capacity in controlled underlay approach outperforms that in another two approaches. The improvement becomes larger as $|\mathcal{N}_m|/|\mathcal{N}_e|$ is larger since femto-BSs achieve higher gain from spatial reuse at macro RBs.

IV. Conclusion

Cross-tier interference in two-tier femtocell networks with co-channel deployment is the main obstacle limiting capacity improvement from spatial reuse. In this work, we have proposed efficient CR solutions for OFDMA-based femtocells to mitigate cross-tier interference. Further, we have derived theoretical results on the downlink capacity of two-tier networks while meeting a per-tier outage constraint under different CR capabilities and allocation approaches at femtocells. Finally, we have proved the essential result that the more information is cognized at femtocells, the more spatial reuse gain can be found.

V. Acknowledgement

This study is conducted under the "Wireless Broadband Communications Technology and Application Project" of the Institute for Information Industry which is subsidized by the Ministry of Economy Affairs of the Republic of China.

References

[1] H. Claussen, "Performance of macro- and co-channel femtocells in a hierarchical cell structure," in *Proc. IEEE PIMRC '07*, Sept. 2007.
[2] D. Lopez-Perez, A. Valcarce, G. de la Roche, and J. Zhang, "OFDMA femtocells: A roadmap on interference avoidance," *IEEE Commun. Mag.*, vol. 47, no. 9, Sept. 2009.
[3] Z. Bharucha, H. Haas, G. Auer, and I. Cosovic, "Femto-cell resource partitioning," in *Proc. IEEE Globecom '09 workshops*, Nov. 2009.
[4] V. Chandrasekhar, M. Kountouris, and J. G. Andrews, "Uplink capacity and interference avoidance for two-tier femtocell networks," *IEEE Trans. Wireless Commun.*, vol. 8, no. 7, pp. 3498–3509, July 2009.
[5] K. Sundaresan and S. Rangarajan, "Efficient resource management in OFDMA femto cells," in *Proc. ACM MobiHoc '09*, May 2009, pp. 33–42.
[6] V. Chandrasekhar, M. Kountouris, and J. G. Andrews, "Coverage in multi-antenna two-tier networks," *IEEE Trans. Wireless Commun.*, vol. 8, no. 10, pp. 5314–5327, Oct. 2009.
[7] S.-Y. Lien and K.-C. Chen, "Cognitive radio resource management for QoS guarantees in autonomous femtocell networks," in *Proc. IEEE ICC '10*, May 2010.
[8] K. Huang, V. Lau, and Y. Chen, "Spectrum sharing between cellular and mobile ad hoc networks: tranmission-capacity trade-off," *IEEE J. Sel. Areas Commun.*, vol. 27, no. 7, Sept. 2009.
[9] L. K. Law, K. Pelechrinis, S. V. Krishnamurthy, and M. Faloutsos, "Downlink capacity of hybrid cellular ad hoc networks," *IEEE/ACM Trans. Netw.*, vol. 18, no. 1, pp. 243–256, Feb. 2010.
[10] S. Srinivasa and S. A. Jafar, "The throughput potential of cognitive radio: A theoretical perspective," *IEEE Commun. Mag.*, vol. 45, no. 5, pp. 73–79, May 2007.
[11] J. Kingman, *Poisson Processes*. Oxford University Press, 1993.
[12] F. Baccelli, B. Blaszczyszyn, and P. Muhlethaler, "An aloha protocol for multihop mobile wireless networks," *IEEE Trans. Inf. Theory*, vol. 52, no. 2, pp. 421–436, Feb. 2006.